

Silencing of desmoplakin decreases connexin43/Na_v1.5 expression and sodium current in HL-1 cardiomyocytes

QIANHUAN ZHANG^{1,2,3}, CHUNYU DENG^{1,2,3}, FANG RAO^{1,2,3}, ROHAN M. MODI⁴,
JIENING ZHU^{2,3}, XIAOYING LIU^{2,3}, LIPING MAI^{2,3}, HONGHONG TAN^{2,3}, XIYONG YU^{1,2,3},
QIUXIONG LIN^{1,2,3}, DINGZHANG XIAO^{2,3}, SUJUAN KUANG^{1,2,3} and SHULIN WU^{1,2,3}

¹Department of Cardiology, Guangdong Cardiovascular Institute; ²Guangdong General Hospital;

³Guangdong Academy of Medical Sciences, Guangzhou, Guangdong 510080, P.R. China;

⁴Department of Pathology, University of Cincinnati College of Medicine, Cincinnati, OH 45267, USA

Received March 6, 2013; Accepted June 12, 2013

DOI: 10.3892/mmr.2013.1594

Abstract. Desmosomes and gap junctions are situated in the intercalated disks of cardiac muscle and maintain the integrity of mechanical coupling and electrical impulse conduction between cells. The desmosomal plakin protein, desmoplakin (DSP), also plays a crucial role in the stability of these interconnected components as well as gap junction connexin proteins. In addition to cell-to-cell junctions, other molecules, including voltage-gated sodium channels (Na_v1.5) are present in the intercalated disk and support the contraction of cardiac muscle. Mutations in genes encoding desmosome proteins may result in fatal arrhythmias, including arrhythmogenic right ventricular cardiomyopathy (ARVC). Therefore, the aim of the present study was to determine whether the presence of DSP is necessary for the normal function and localization of gap junction protein connexin43 (Cx43) and Na_v1.5. To examine this hypothesis, RNA interference was utilized to knock down the expression of DSP in HL-1 cells and the content, distribution and function of Cx43 and Na_v1.5 was assessed. Western blotting and flow cytometry experiments revealed that Cx43 and Na_v1.5 expression decreased following DSP silencing. In addition, immunofluorescence studies demonstrated that a loss of DSP expression led to an abnormal distribution of Cx43 and Na_v1.5, while scrape-loading dye/transfer revealed a decrease in dye transfer in DSP siRNA-treated cells. The sodium current was also recorded by the whole-cell patch clamp technique. The results indicated that DSP suppression decreased sodium current and slowed conduction velocity in cultured cells. The

present study indicates that impaired mechanical coupling largely affects electrical synchrony, further uncovering the pathogenesis of ARVC.

Introduction

Individual cardiomyocytes are connected to each other via three cell-cell junctions, desmosomes (macula adherens), adherens junctions (fascia adherens) and gap junctions which collectively make up intercalated disks. These membrane junctions ensure mechanical coupling between cells and enable the propagation of electrical impulses through cardiac muscles to propel muscle contraction (1).

Desmosomes are of particular interest as they bear a high mechanical load and are particularly abundant in the heart. Desmoplakin (DSP), a member of the plakin family, is an extremely large desmosomal protein that serves as an intracellular link between desmosomes and intermediate filaments. A wide array of mutations in the DSP protein have been observed in individuals with arrhythmogenic right ventricular cardiomyopathy (ARVC) (2-4). A mutation in the DSP protein has been suggested to disrupt various cell targets, resulting in abnormal protein interactions at intercellular junctions. This process may ultimately lead to electrical dysfunction, with the possibility of life-threatening arrhythmias and sudden cardiac death (5).

While the mutated proteins in ARVC may lead to the loss of desmosomal integrity, this observation does not account as to why life-threatening arrhythmias occur early in the course of the disease before cardiomyocytes are replaced by fibro-fatty tissue. The mechanical functions of desmosomes in heart tissue depend on complex binding interactions between multiple proteins. Disruption of cell junctions associated with desmosomal protein mutations is considered to affect the structure and function of electrical connections at gap junctions, which may contribute to impairment in cardiac electrical conduction and associated arrhythmias. Structurally, the gap junction consists of two hemichannels or connexons and the principal subtype in the human heart is connexin43 (Cx43) (6). Of note, the correlation between DSP and gap junctions in cardiac arrhythmias has not been investigated.

Correspondence to: Dr Shulin Wu, Department of Cardiology, Guangdong General Hospital, Guangdong Cardiovascular Institute, Guangdong Academy of Medical Sciences, 96 Dongchuan Road, Guangzhou, Guangdong 510080, P.R. China
E-mail: guangzhou_shulin_wu2012@hotmail.com

Key words: connexin43, desmoplakin, sodium current, arrhythmogenic right ventricular cardiomyopathy, small interfering RNA

Apart from cell-cell junctions, other molecules that reside in the intercalated disk include voltage-gated sodium channels. A previous study indicated that Na_v1.5, the major α -subunit of the cardiac sodium channel, is situated in the intercalated disk (7). Na_v1.5 is responsible for rapid depolarization of intercalated disks and is important for action potential propagation. In addition, while Na_v1.5 may be involved in the occurrence of arrhythmias in patients with ARVC (8-10), no studies have currently shown Na_v1.5 to be involved in ventricular arrhythmias due to desmosomal protein mutations.

In the present study, the potential link between DSP desmosomal protein expression and the impact it may have on Cx43 and Na_v1.5 was investigated. To test this hypothesis, the study was designed to explore the distribution and function of gap junctions and Na_v1.5 while inhibiting the expression of DSP in HL-1 cardiomyocytes.

Materials and methods

Preparation of HL-1 cardiomyocytes. HL-1 cells are a cardiac muscle cell line derived from AT-1 mice that have the ability to be continuously passaged. These cells accurately represent the electrophysiological functioning of adult cardiomyocytes *in vitro*, making them ideal for the current study (11,12). HL-1 cells were obtained from the laboratory of William Claycomb (Louisiana State University Health Science Center, New Orleans, LA, USA) and were maintained as previously described (11). HL-1 cells were grown in Claycomb medium (JRH Biosciences, Lenexa, KS, USA), supplemented with 10% v/v fetal bovine serum (JRH Biosciences), 100 mM norepinephrine (Sigma-Aldrich, St. Louis, MO, USA), 4 mM L-glutamine and 1% penicillin/streptomycin (Invitrogen Life Technologies, Carlsbad, CA, USA) in a humidified 5% CO₂ incubator at 37°C. Culture flasks, dishes and plates were precoated with 1 μ g/cm² fibronectin/0.02% w/v gelatin solution (Sigma-Aldrich). The medium was changed every 24-48 h.

Small interfering RNA (siRNA) transfection. siRNA specific for mouse and control desmoplakin (NM_0238422) were purchased from GenePharma (Shanghai, China). The sequence for targeting and negative control siRNA contained the following four polynucleotides (sense sequences only): 5'-GCACCAGCAGGACGUUCUATT-3'; 5'-CGAUCAGAU GGAAAUCAUATT-3'; 5'-GGAGCGACAAGAACACCA ATT-3' and 5'-UUCUCCGAACGUGUCUCGUTT-3' (negative control). The transfection procedure was performed according to the manufacturer's instructions with Lipofectamine 2000[®] reagent (Invitrogen Life Technologies). Transfection was performed on 1-2x10⁵ cells/well in 6-well plates in serum- and antibiotic-free cell culture medium. Cells were washed in Opti-MEM (Invitrogen Life Technologies) twice prior to the addition of 2 ml serum-free culture medium. Then, 500 μ l mixed Opti-MEM, siRNA of negative control or desmoplakin and Lipofectamine 2000 (5 μ l/well) were added into each well to a final siRNA concentration of 50 nM. The medium was changed the following day and cells were used experimentally 48-120 h following transfection.

Western blotting. HL-1 cells in 6-well plates were rinsed twice with PBS and then added to 100 μ l RIPA lysis buffer and

complete protease inhibitor (Roche Diagnostics, Mannheim, Germany). The plates were agitated for 15 min at 4°C and centrifuged at 14,800 x g for 20 min. Protein concentrations were determined and 30 μ g samples were diluted with 4X loading buffer (Invitrogen Life Technologies) and heated at 95°C for 5 min. Next, 10 μ l 4X SDB was added to 30 μ l sample, run in a 4-12% Bis-Tris precast gel (Invitrogen Life Technologies) and transferred to nitrocellulose membranes (Amersham Pharmacia Biotech, Piscataway, NJ, USA) according to the manufacturer's instructions. Membranes were blocked in dried skimmed milk powder in Tween 20 Tris-buffered saline for 2 h at room temperature prior to overnight incubation at 4°C with the following primary antibodies: mouse anti-desmoplakin I/II (1:200; Abcam, Cambridge, UK), rabbit anti-desmoplakin I/II (1:200; Santa Cruz Biotechnology Inc., CA, USA), rabbit anti-Cx43 (1:500; Cell Signaling Technology, Inc, Danvers, MA, USA) and rabbit polyclonal anti-Na_v1.5 (1:100; Alomone Labs, Jerusalem, Israel). Anti-GAPDH (1:1,000; Zymed Laboratories, Carlsbad CA, USA) was used as the loading control. The secondary antibody against mouse primary antibodies was goat anti-mouse IgG-HRP (1:5,000), while the secondary antibody used against rabbit primary antibodies was goat anti-rabbit IgG-HRP (1:5,000; Santa Cruz Biotechnology Inc.). Protein bands were visualized using electrochemiluminescence reagents (Invitrogen Life Technologies). The images were evaluated densitometrically using Gel-Pro Analyzer 4.0 software (Media Cybernetics, Inc., Rockville, MD, USA).

Flow cytometry. HL-1 cells were routinely dissociated with trypsin/EDTA which was pre-warmed to 37°C. For intracellular protein labeling, the cells were fixed and permeabilized according to the manufacturer's instructions by Fix and Perm Cell Reagent (MultiSciences Biotech Co., Ltd., Shanghai, China). The cells were fixed in 100 μ l fixation reagent for 15 min at room temperature, washed in PBS and then resuspended in 100 μ l permeabilization reagent for 20 min at room temperature together with the primary antibodies: mouse anti-desmoplakin I/II, rabbit anti-connexin 43 and rabbit polyclonal to Na_v1.5. After washing the cells the following secondary antibodies were added: Alexa Fluor 488 goat anti-rabbit IgG (Invitrogen Life Technologies) and goat anti-mouse IgG-PE (MultiSciences Biotech). The mixtures were incubated for 20 min at room temperature. Following a final wash, the cells were resuspended in PBS and then analyzed using flow cytometry (Beckman Coulter Inc., Brea, CA, USA). Alexa Fluor 488 IgG or IgG-PE staining alone was used as the negative control.

Immunofluorescent staining and laser scanning confocal microscopy. siRNA-transfected cells, cells treated with transfection reagent only and untreated cells were all grown on collagen-coated coverslips, rinsed twice in PBS and fixed with methanol at -20°C for 20 min. Following fixation, the coverslips were directly washed in PBS for 5 min, followed by incubation with PBS, 0.2% Triton X-100 and 5% bovine serum albumin for 20 min at room temperature. Following rinsing with PBS, the cells were incubated with primary antibody at 4°C in a humidity box. Cx43, desmoplakin and Na_v1.5 proteins were examined following incubation with mouse anti-desmo-

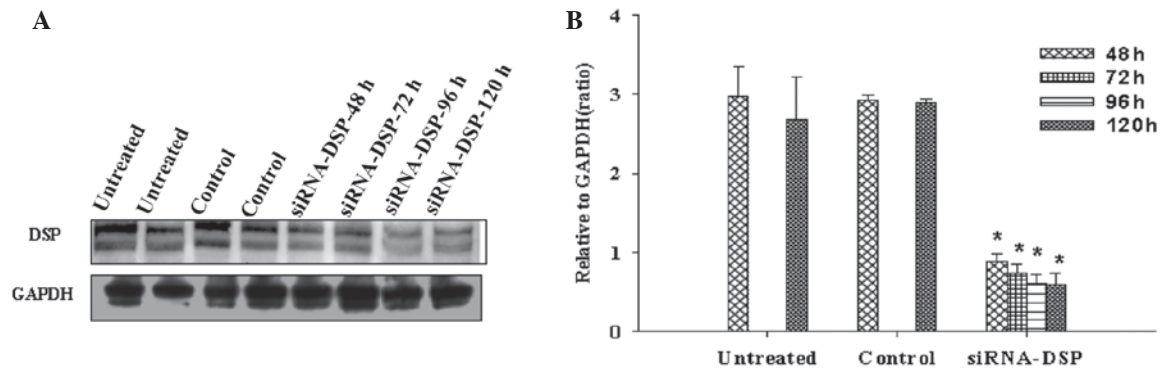


Figure 1. Western blot analysis of DSP or GAPDH (bottom bands) expression in HL-1 cells. (A) Representative western blot analysis of DSP levels in cell lysates untreated or infected with DSP siRNA or non-targeting siRNA. Cells at 48, 72, 96 and 120 h culture were compared with the initial cells. GAPDH was used as an internal control. A marked downregulation of DSP following DSP siRNA treatment was observed. (B) Densitometric analysis of DSP protein levels in untreated and infected cells with DSP siRNA or non-targeting siRNA. DSP, desmoplakin; siRNA, small interfering RNA.

plakin I/II (1:200; Abcam), rabbit anti-Cx43 (1:200; CST) and rabbit polyclonal to $\text{Na}_v1.5$ (1:200; Alomone). Coverslips were subsequently washed 3 times with PBS and incubated with the corresponding secondary antibodies for 2 h at room temperature in a dark, humid box. Secondary antibodies included Alexa Fluor 647 goat anti-mouse (Invitrogen Life Technologies) and Alexa fluor 488 goat anti-rabbit (Invitrogen Life Technologies) diluted to 1:500 in blocking buffer. DAPI staining was then performed to identify nuclei. Following a final rinsing step, coverslips were mounted using antifade mounting media (Applygen Technologies Inc, Beijing, China). Cardiomyocytes were observed at 48, 72, 96 and 120 h following incubation with siRNAs targeting desmoplakin, with non-targeting siRNAs or with transfection reagent only and were compared with untreated control cells at each time point.

Scrape loading dye transfer. The functions of gap junctional intercellular communication in adjacent cells were assessed by scrape loading dye transfer (SLDT) with fluorescent dye Lucifer Yellow (LY; Sigma-Aldrich). At 90% confluence, the cultured cells were rinsed three times with PBS. A cross scrape through the monolayer was made using a surgical scalpel, followed by incubation with 100 g/l LY in 0.33 mol/l LiCl for 3 min in a dark room at room temperature and several PBS washes to remove any background fluorescence. Cells were then fixed with 4% paraformaldehyde and the optical density was detected using confocal laser scanning microscopy (Leica, Wetzlar, Germany).

Electrophysiology. HL-1 cells were isolated from culture dishes following infection with siRNA targeting desmoplakin or with non-targeting siRNA for 5 days. Whole cell cardiac sodium current (I_{Na}) was recorded from HL-1 cells. Recorded cells were rod-shaped and appeared striated. Cells were perfused with extracellular solution containing: 136 mM NaCl, 1 mM MgCl_2 , 1 mM CaCl_2 , 0.5 mM CoCl, 10 mM HEPES, 0.33 mM NaH_2PO_4 , 5.4 mM CsCl and 10 mM glucose (pH 7.3). The pipette solution contained: 20 mM CsCl, 110 mM CsF, 5 mM NaCl, 10 mM HEPES, 5 mM Na_2ATP , 1mM MgCl and 10 mM EGTA (pH 7.2). Pipette resistances were 2-3 M Ω . Access resistance was compensated to 1-2 M Ω . Recordings were performed using an Axopatch 200B amplifier and data

acquisition and analysis were performed using the Digidata 1200B-pClamp 7.0 data-acquisition system (Axon Instruments, Jakarta, Indonesia). Signals were filtered at 5 kHz and stored on a computer. All experiments were performed at room temperature. To characterize the voltage dependence of the peak I_{Na} , single cells were held at -120 mV and 200 msec voltage steps were applied from -90 to +30 mV in 5 mV increments. The interval between voltage steps was 3 sec. Voltage-dependence of inactivation was assessed by holding cells at various potentials between -130 and -40 mV followed by a 30 msec test pulse to -40 mV to elicit I_{Na} . Recovery from inactivation was studied by holding cells at -120 mV and applying two 20 msec test pulses (S1, S2) to -40 mV separated by increasing increments of 2 msec to a maximum S1-S2 interval of 80 msec. The S1-S1 interval was maintained at 3 sec. Data are presented as mean \pm SEM.

Results

HL-1 cells treated with DSP siRNA exhibit downregulation of DSP. DSP siRNA was introduced into HL-1 cells *in vitro* to investigate the effect of loss of DSP expression on the function and distribution of Cx43/ $\text{Na}_v1.5$. Initially, DSP mRNA expression levels in HL-1 cells were assessed by real-time PCR analysis following transfection with DSP siRNA. GAPDH was used as the internal control. Three distinct siRNA sequences decreased levels of DSP mRNA expression; DSP mRNA levels were decreased by >70% from the control using a pair of DSP mRNA sequences (5'GGAGCGACAAGAACACCAATT3', sense sequence). Subsequent experiments were conducted using this DSP siRNA sequence.

Western blot analysis following treatment with DSP siRNA consistently revealed a significantly reduced expression of DSP in HL-1 cells when compared with untreated and non-targeting siRNA control treatments (GAPDH was used as a loading control; n=3). Fig. 1 shows that DSP reduction persisted between 48 and 120 h. For quantification, each band density was measured relative to its corresponding GAPDH control.

Quantification of immunoblot signals revealed that the expression of DSP protein was markedly reduced following 48-120 h DSP siRNA treatment compared with control siRNA or untreated cells.

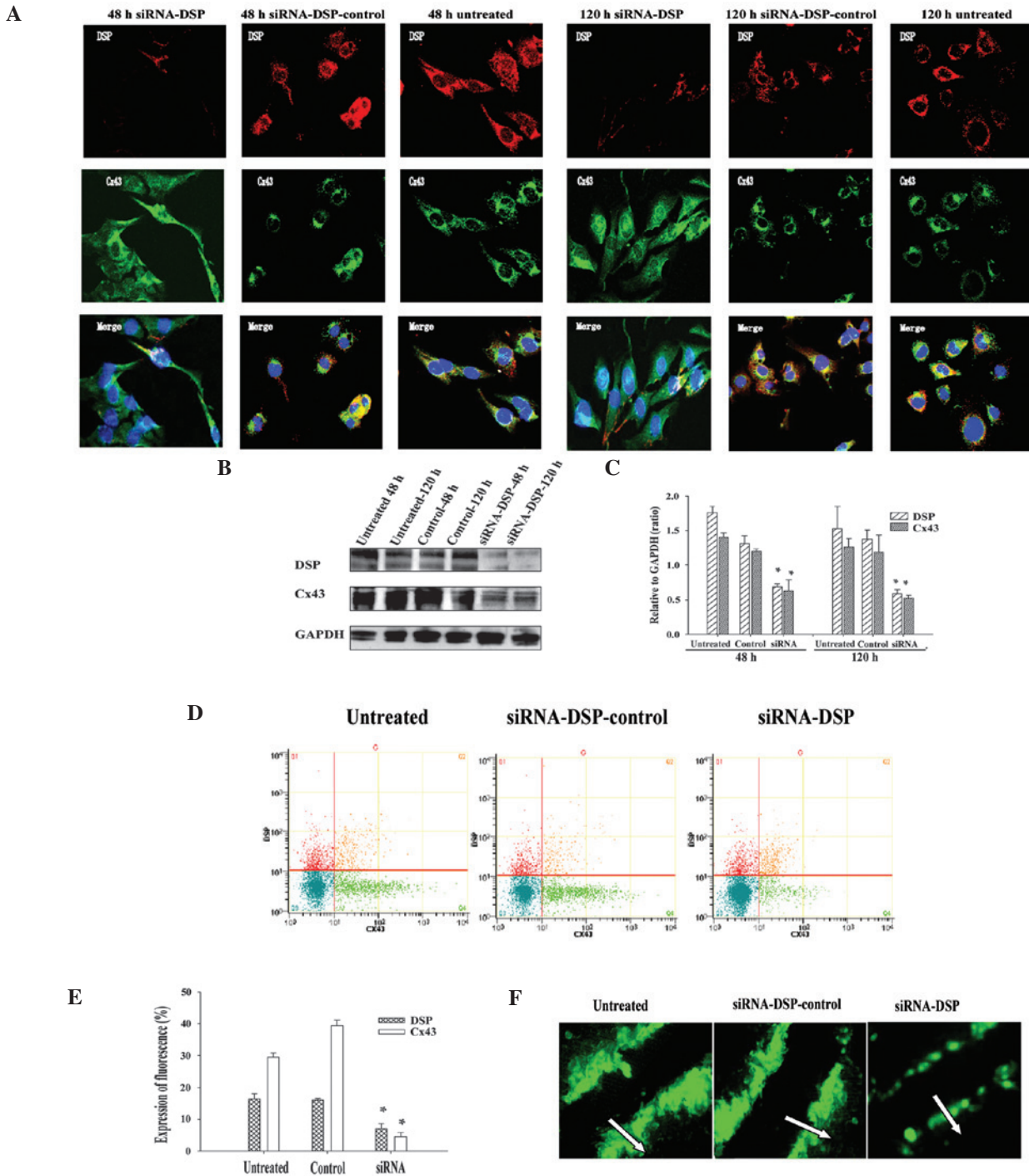


Figure 2. Effect of DSP siRNA on the structure and function of the gap junction. (A) Immunofluorescence microscopy of HL-1 cell cultures treated for 48 or 120 h with DSP siRNA, non-targeting control siRNA or without any siRNA. DSP siRNA-treated cells as observed following immunostaining for DSP (red) and Cx43 (green). The corresponding merger images, in combination with nuclear DAPI staining (blue) are shown in the bottom panel. Notably, the loss of DSP expression and significant redistribution of Cx43 in DSP siRNA-treated cells. (B and C) Western blot analysis and the correlated densitometry for DSP and Cx43 under the same conditions used for (A). (D and E) Flow cytometry and the correlated quantification analysis of HL-1 cell cultures treated for 120 h revealed the same results as (B). (F) SLDT analysis of the coupling between cultured HL-1 cells. White arrow indicates the distance of dye transfer. DSP, desmoplakin; siRNA, small interfering RNA; Cx43, connexin43; SLDT, scrape loading dye transfer.

DSP siRNA alters Cx43 expression and function in HL-1 cells

Effect of DSP silencing on content and distribution of Cx43. Results of immunolocalization of Cx43 and DSP in HL-1 cells indicated that Cx43 undergoes progressive and marked reorganization following DSP siRNA silencing. These effects were not detected with non-targeting control siRNA (control

siRNA) and untreated cells. Fig. 2A shows typical results observed at the first (48 h) and last (120 h) time-points following transfection with DSP siRNA, compared with control siRNA or untreated cells. Colocalization to the site of cell-cell contact was apparent in untreated conditions and when cells were infected with non-targeting control siRNA. The content of Cx43 at the cell-cell borders was significantly distributed in

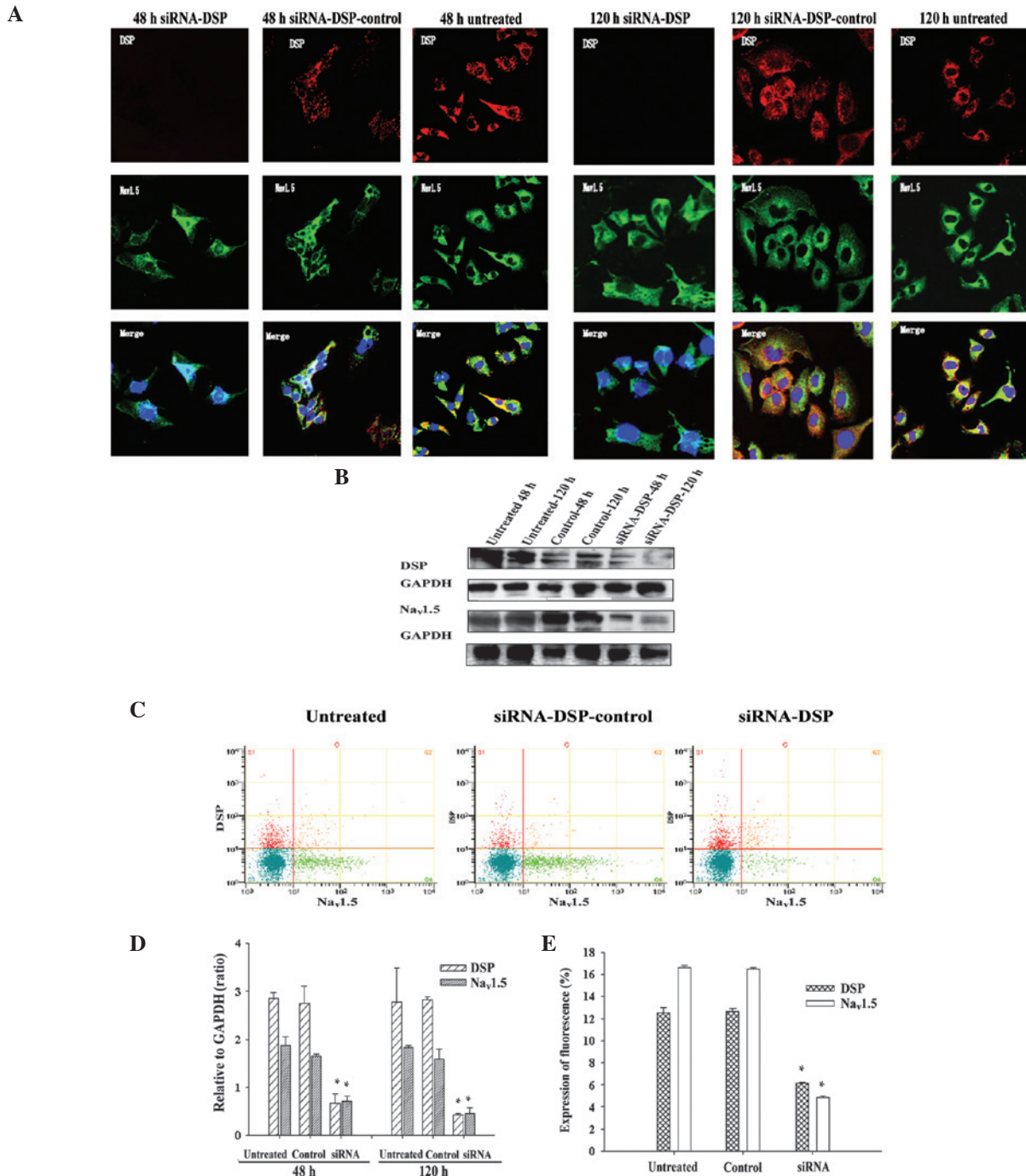


Figure 3. Effect of DSP siRNA on the structure of $\text{Na}_v1.5$ and sodium current. (A) Immunofluorescence microscopy of HL-1 cell cultures treated for 48 or 120 h with DSP siRNA, non-targeting control siRNA or without any siRNA. DSP siRNA-treated cells as observed following immunostaining for DSP (red) and $\text{Na}_v1.5$ (green). The corresponding merger images, in combination with nuclear DAPI staining (blue) are shown in the bottom panel. A decrease in DSP expression and significant redistribution of $\text{Na}_v1.5$ in DSP siRNA treated cells was observed. (B) Western blot analysis for DSP and $\text{Na}_v1.5$ under the same conditions used for (A). (C) Flow cytometry of HL-1 cell cultures treated for 120 h revealed the same results as (B). DSP, desmoplakin; siRNA, small interfering RNA.

transfected cells, as Cx43 was identified within the intracellular space. In addition, Cx43 protein expression levels were investigated using western blot analysis. Cx43 protein content was reduced following DSP knockdown by DSP siRNA (Fig. 2B). Quantitative evaluations of the density of the Cx43 signal also revealed that the Cx43 level was markedly reduced following 48-120 h DSP siRNA treatment compared to control siRNA or untreated cells. To clarify Cx43 expression in HL-1 cells treated with DSP siRNA, levels of Cx43 fluorescence were

measured by flow cytometry. It was observed that the rate of Cx43 fluorescence expression detected in HL-1 cells treated with DSP mRNA was decreased when compared with control siRNA or untreated cells (Fig. 2C and D). Overall, these results suggest that a loss of DSP expression leads to a significant decrease and redistribution of Cx43.

Changes in the function of gap junctions in DSP-silenced cells. To determine whether the loss of DSP expression affected the function of gap junctions between cell pairs, the transfer

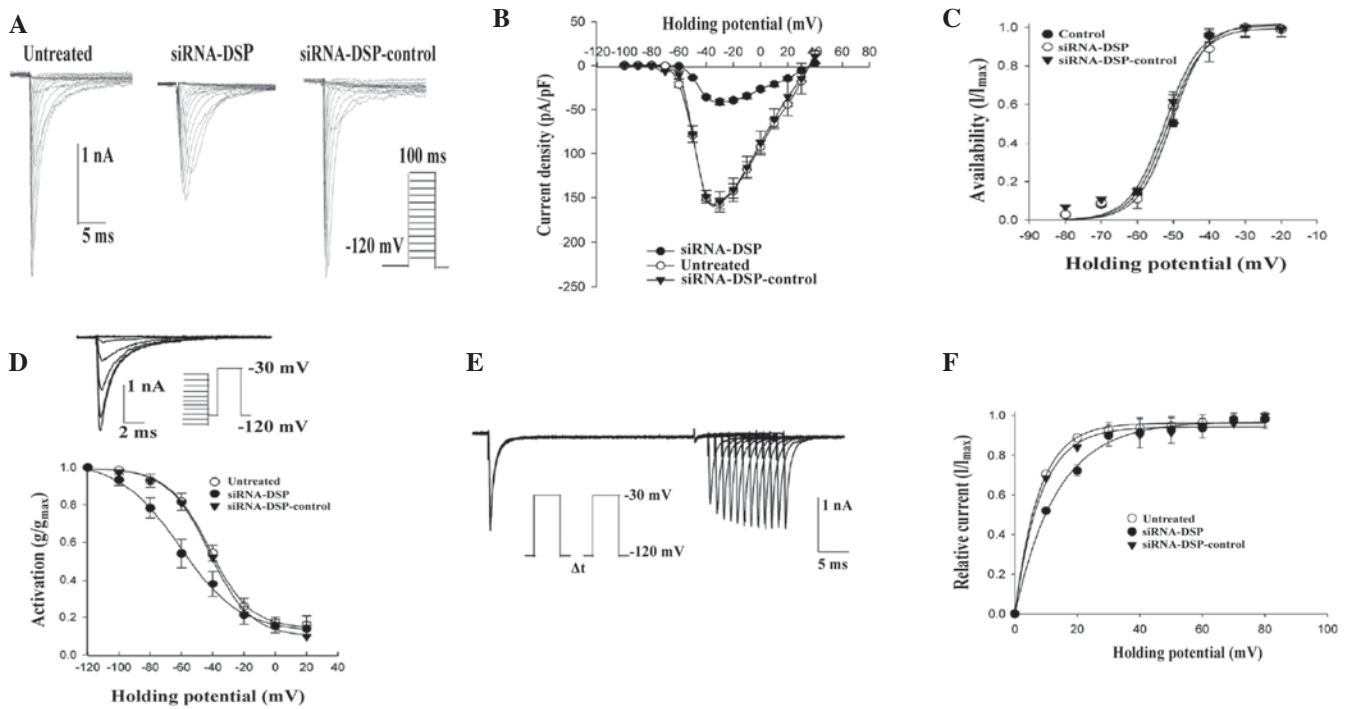


Figure 4. Voltage clamp data from adult cardiomyocytes following DSP knockdown. Cells untreated or treated with non-targeting siRNA were used as the control. (A) Currents elicited by increasing voltage steps from a holding potential of -120 mV. (B) Mean amplitude of peak inward current density as a function of membrane potential during same voltage steps as in (A). (C and D) Voltage dependence of steady-state inactivation. (E and F) Time course of recovery from inactivation. DSP, desmoplakin; siRNA, small interfering RNA.

of LY across gap junctions in adjacent cells was assessed by SLDT. The distance over which LY spread in the cells treated with DSP siRNA was significantly decreased compared with the control siRNA or untreated cells (Fig. 2E).

DSP siRNA affects Na_v1.5 expression and sodium currents in HL-1 cells

DSP siRNA alters Na_v1.5 expression in HL-1 cells. To characterize the effects of DSP siRNA on Na_v1.5, immunofluorescent experiments were performed in transfected HL-1 cells. Results of the immunofluorescence experiments suggested that Na_v1.5 undergoes significant alterations following treatment with DSP siRNA, which were not observed with non-targeting control siRNA and untreated cells (Fig. 3A). The expression of Na_v1.5 at the cell-cell borders was markedly reduced in transfected cells (Fig. 3A, left panel), while residual Na_v1.5 protein tended to relocate in the cytoplasmic space. Colocalization of Na_v1.5 and DSP proteins at cell borders was observed in HL-1 cells infected with non-targeting control siRNA (Fig. 2A, middle panel) and untreated conditions (Fig. 3A, left panel). Western blotting and flow cytometry measuring the expression of DSP siRNA and Na_v1.5 protein revealed that the Na_v1.5 protein content was reduced following DSP siRNA silencing. The rate of Cx43 fluorescence expression in HL-1 cells treated with DSP mRNA was decreased compared with control siRNA or untreated cells. The results of immunofluorescence, western blotting and flow cytometry suggested that DSP siRNA silencing has a deleterious effect on Na_v1.5 localization and expression.

Effect of DSP siRNA on sodium currents in HL-1 cells.

The properties of I_{Na} as a function of DSP expression were assessed and sodium currents were recorded using a voltage clamp. Fig. 4A shows an example of currents obtained from

cells untreated or treated with an oligonucleotide mixture. Composite data are presented in Fig. 4B-F. Treatment with control siRNA did not affect the current parameters. However, a decrease in peak current density (Fig. 4B), a shift in voltage dependent steady-state inactivation (Fig. 4D) and a prolongation of time-dependent recovery from inactivation (Fig. 4F) were observed in DSP-silenced cells.

Discussion

It has been well documented that DSP is a major component of desmosomes and plays a significant role in the maintenance of cardiac tissue integrity. Previous studies have proposed that DSP and plakophilin 2 (PKP2) interact with each other at their N-terminal domains (13). Previously, Oxford *et al* demonstrated that Cx43 and PKP2 may coexist in the same macromolecular complex (6). The present study expands this concept by demonstrating that a loss of DSP leads to a decreased expression and redistribution of Cx43 protein. This phenomenon has a significant impact on gap junction function and reveals a reduction in the distance of LY spread from cell to cell. The current observations are the first to clearly demonstrate an association between DSP downregulation and abnormal cell-to-cell communication mediated by Cx43. The observations indicate that DSP may have a greater impact on regulating the formation and interaction of mechanical and electrical junctional complexes than previously hypothesized.

Gap junctions are intercellular channels that connect adjacent cells via the cytoplasm. Previous studies have indicated that the disruption of desmosomal proteins results in a strong effect on the integrity or stability of the gap junction (1). Carvajal syndrome is a cardiomyopathy caused by a mutation

in DSP that is characterized by distinct ultrastructural abnormalities of the intercalated disk (5). Thus, the mutation in DSP may not only interfere with molecular interactions among the desmosomal proteins, but also cause contractile- and electrical- related dysfunctions.

A previous study identified other proteins localized at the intercalated disk that interconnected with Cx43 (14). While the functional role of these protein-protein interactions has not been clearly established, it has been hypothesized that they are important in coupling between inter- and intracellular signaling in the heart. The current study reveals that loss of DSP expression leads to Cx43 remodeling. Notably, loss of the DSP signal may be associated with the change in the integrity of DSP-Cx43 interactions and the heterozygous deletion of DSP in mice ultimately led to fibro-fatty infiltration. While gap junction plaques do not define the location of all gap junctions, a decrease in cell-cell dye coupling was observed. Based on these observations, it was suggested that DSP and Cx43 represent a molecular network that may be disrupted by an ARVC relevant mutation. In human DSP mutation carriers, there was a significant conduction delay at short coupling intervals with no evidence of fibro-fatty replacement, despite a downregulation in cardiac Cx43 protein expression. Therefore, future studies must determine the manner in which Cx43 relocalization prior to major structural and histological changes affects development in animal models as well as patients.

Little is known concerning the signaling correlations between cell-cell junctions and the voltage-gated sodium channel in cardiac cells. Voltage-dependent sodium channels are responsible for generating action potentials and the rapid conduction of electrical signals in excitable cells (15). While it has been observed that a mutation in Na_v1.5 may cause cardiac arrhythmias and sudden cardiac death, it is not yet clear how mutations in Na_v1.5 are responsible for such a large spectrum of diseases along with the overlapping syndromes (16). Gomes *et al* (17) previously demonstrated that sodium channels localize to the intercalated disk in the biopsy samples of an ARVC patient, potentially contributing to a reduced conduction velocity. It was suggested that a loss of DSP expression would significantly affect propagation properties in cardiomyocytes due to the change in sodium current function. The current study effectively demonstrates that loss of DSP leads to a decreased expression and redistribution of the Na_v1.5 protein and knockdown of DSP expression decreases the sodium current while also slowing the conduction velocity in cultured HL-1 cells. However, it is important to emphasize that the present observations do not disprove a possible effect of DSP silencing on the membrane and other unrelated factors may have affected the slow conduction velocity in the current experiments. Future investigations are likely to be directed towards addressing this possibility.

Mutations in DSP have been observed to be the main cause of ARVC that presents with clinical manifestations, including ventricular arrhythmias and sudden death under strenuous circumstances (2,18). The underlying mechanisms by which mutations in cell-cell junction proteins affect electric synchrony remains undefined.

Results of the current study indicate a correlation between three components of the intercalated disk, desmosomes, gap junctions and the voltage-gated sodium channel Na_v1.5

complex. This is the first association identified between DSP expression and function of the sodium channel complex, demonstrating that the molecular integrity of mechanical connections may be associated with sodium channel function. Additional studies are required to understand the pathogenesis of ventricular arrhythmias in ARVC. However, current observations are likely to be a stepping stone towards identification of a treatment for ARVC patients.

Acknowledgements

The study was supported by grants from Guangdong Nature Science Foundation to Shulin Wu (no. 10151008002000011).

References

- Noorman M, van der Heyden MA, van Veen TA, *et al*: Cardiac cell-cell junctions in health and disease: Electrical versus mechanical coupling. *J Mol Cell Cardiol* 47: 23-31, 2009
- Bauce B, Basso C, Rampazzo A, *et al*: Clinical profile of four families with arrhythmogenic right ventricular cardiomyopathy caused by dominant desmoplakin mutations. *Eur Heart J* 26: 1666-1675, 2005.
- Rampazzo A, Nava A, Malacrida S, *et al*: Mutation in human desmoplakin domain binding to plakoglobin causes a dominant form of arrhythmogenic right ventricular cardiomyopathy. *Am J Hum Genet* 71: 1200-1206, 2002.
- Norman M, Simpson M, Mogensen J, *et al*: Novel mutation in desmoplakin causes arrhythmogenic left ventricular cardiomyopathy. *Circulation* 112: 636-642, 2005.
- Kaplan SR, Gard JJ, Carvajal-Huerta L, *et al*: Structural and molecular pathology of the heart in Carvajal syndrome. *Cardiovasc Pathol* 13: 26-32, 2004.
- Oxford EM, Musa H, Maass K, *et al*: Connexin43 remodeling caused by inhibition of plakophilin-2 expression in cardiac cells. *Circ Res* 101: 703-711, 2007.
- Roden DM, Balsler JR, George AL JR and Anderson ME: Cardiac ion channels. *Annu Rev Physiol* 64: 431-475, 2002.
- Abriel H: Cardiac sodium channel Na_v1.5 and interacting proteins: Physiology and pathophysiology. *J Mol Cell Cardiol* 48: 2-11, 2010.
- Peters S, Trümmel M, Denecke S and Koehler B: Results of ajmaline testing in patients with arrhythmogenic right ventricular dysplasia-cardiomyopathy. *Int J Cardiol* 95: 207-210, 2004.
- Peters S: Arrhythmogenic right ventricular dysplasia-cardiomyopathy and provokable coved-type ST-segment elevation in right precordial leads: clues from long-term follow-up. *Europace* 10: 816-820, 2008.
- Chaudary N, Shuralyova I, Liron T, *et al*: Transport characteristics of HL-1 cells: A new model for the study of adenosine physiology in cardiomyocytes. *Biochem Cell Biol* 80: 655-665, 2002.
- Clayton WC, Lanson NA Jr, Stallworth BS, *et al*: HL-1 cells: A cardiac muscle cell line that contracts and retains phenotypic characteristics of the adult cardiomyocyte. *Proc Natl Acad Sci USA* 95: 2979-2984, 1998.
- Stokes DL: Desmosomes from a structural perspective. *Curr Opin Cell Biol* 19: 565-571, 2007.
- Shaw RM, Fay AJ, Puthenveedu MA, *et al*: Microtubule plus-end-tracking proteins target gap junctions directly from the cell interior to adherens junctions. *Cell* 128: 547-560, 2007.
- Plaisier AS, Burgmans MC, Voncken EP, *et al*: Image quality assessment of the right ventricle with three different delayed enhancement sequences in patients suspected of ARVC/D. *Int J Cardiovasc Imaging* 28: 595-601, 2011.
- Derangeon M, Montnach J, Baró I and Charpentier F: Mouse models of SCN5A-related cardiac arrhythmias. *Frontiers Physiol* 3: 210, 2003.
- Gomes J, Finlay M, Ahmed AK, *et al*: Electrophysiological abnormalities precede overt structural changes in arrhythmogenic right ventricular cardiomyopathy due to mutations in desmoplakin-a combined murine and human study. *Eur Heart J* 33: 1942-1953, 2012.
- Delmar M and McKenna WJ: The cardiac desmosome and arrhythmogenic cardiomyopathies: from gene to disease. *Circ Res* 107: 700-714, 2010.